

Gastrointestinal, Hepatobiliary and Pancreatic Pathology

Up-Regulation of Telomere-Binding Proteins, TRF1, TRF2, and TIN2 Is Related to Telomere Shortening during Human Multistep Hepatocarcinogenesis

Bong-Kyeong Oh,* Young-Joo Kim,*
Chanil Park,*† and Young Nyun Park*†

From the Department of Pathology,* Center for Chronic Metabolic Disease Research and Brain Korea 21 Project for Medical Science, and the Institute of Gastroenterology,† Yonsei University College of Medicine, Seoul, Korea

The telomeric repeat-binding factor 1 (TRF1), TRF2, and the TRF1-interacting nuclear protein 2 (TIN2) are involved in telomere maintenance. We describe the regulation of expression of these genes along with their relationship to telomere length in hepatocarcinogenesis. The transcriptional expression of these genes, TRF1 protein, and telomere length was examined in 9 normal livers, 14 chronic hepatitis, 24 liver cirrhosis, 5 large regenerative nodules, 14 low-grade dysplastic nodules (DNs), 7 high-grade DNs, 10 DN with hepatocellular carcinoma (HCC) foci, and 31 HCCs. The expression of TRF1, TRF2, TIN2 mRNA, and TRF1 protein was gradually increased according to the progression of hepatocarcinogenesis with a marked increase in high-grade DN and DN with HCC foci and a further increase in HCCs. There was a gradual shortening of telomere during hepatocarcinogenesis with a significant reduction in length in DN. Most nodular lesions (52 of 67) had shorter telomeres than their adjacent chronic hepatitis or liver cirrhosis, and the telomere lengths were inversely correlated with the mRNA level of these genes ($P \leq 0.001$). This was more evident in DN and DN with HCC foci. In conclusion, TRF1, TRF2, and TIN2 might be involved in multistep hepatocarcinogenesis by playing crucial roles in telomere shortening. (*Am J Pathol* 2005, 166:73–80)

Telomeres, which are located at the end of a chromosome, are composed of the 3'-end overhang of G-strand, the double strand of telomeric DNA, and telomere-binding proteins.^{1–4} The telomeres stabilize the natural end of the chromosome, protect it from end-to-end fusion and

mediate chromosome pairing during cell division.^{5–7} When telomeres reach a critically short length, primary cells stop dividing and enter senescence. In contrast, most transformed cells including cancer cells maintain short but stable telomeres by activating telomerase. Therefore, the telomere maintenance along with telomerase activation has been suggested as a general mechanism of tumorigenesis.⁸

Telomeres are known to form a loop structure or a t-loop as a result of an invasion of the single-stranded G-tail into the double-stranded telomeric tract.⁹ The telomeric repeat-binding factor (TRF) 1 and TRF2 directly bind to the double-stranded region of the telomere and play important roles in the t-loop structure.¹⁰ Growing evidence has shown that these proteins are involved in telomere maintenance by acting as negative regulators. TRF1 negatively regulates the telomere length by limiting the access of telomerase to the telomere and mediates the interaction of the telomere with a mitotic spindle.^{11,12} TRF2 overexpression leads to the progressive shortening of the telomere length, and the inhibition of TRF2 induces growth arrest.¹³ TRF1-interacting protein 2 (TIN2) colocalizes with TRF1 in the nucleus. A TIN2 mutant extends telomeres in telomerase-positive cells,¹⁴ suggesting that TIN2 also controls the telomere length. Manipulation of the telomere-binding protein gene expression reveals that alterations in those proteins can impair the function of the telomere and induce senescence.^{9,12,14–16} Several reports have described the up-regulation of TRF1, TRF2, and TIN2 in lung cancer,¹⁷ gastric cancer,¹⁸ and that of TRF2 in lymphomas.¹⁹ In contrast, down-regulation of these genes has been reported in breast cancers,²⁰ gastric cancers,²¹ and malignant hematopoietic cells.²²

Hepatocellular carcinoma (HCC) is the seventh most common cancer and accounts for the highest number of

Supported by the Basic Research Program of the Korea Science and Engineering Foundation (grant no. R13-2002-054-01005-0).

Accepted for publication September 10, 2004.

Address reprint requests to Young Nyun Park, M.D., Ph.D., Department of Pathology, and Brain Korea 21 Project for Medical Science, Yonsei University College of Medicine, CPO Box 8044, Seoul, Korea. E-mail: young0608@yumc.yonsei.ac.kr.

adult malignancies in those areas endemic for the hepatitis B virus. There is increasing evidence of a multistep process in human hepatocarcinogenesis, emphasizing the preneoplastic nature of large nodules, which are referred as dysplastic nodules (DNs) or adenomatous hyperplasia, usually found in a cirrhotic liver.²³ DN, especially high-grade DN, are believed to be preneoplastic lesions, although the nature of low-grade DN appears less resolved than that of high-grade DN.

Telomere shortening and telomerase activation, which are important for carcinogenesis, have been observed in HCCs.^{24–29} A previous study demonstrated that telomere shortening and telomerase activation occur in DN during the early stages of hepatocarcinogenesis with a significant change in the transition of low-grade DN to high-grade DN.³⁰ However, the expression levels of telomeric repeat-binding proteins as well as their relationship with the telomere length during multistep hepatocarcinogenesis have not been examined. To address these issues, the mRNA levels of TRF1, TRF2, and TIN2, as well as the TRF1 protein expression level, were examined using real-time quantitative reverse transcriptase (RT)-polymerase chain reaction (PCR) and immunohistochemistry, respectively, in normal livers, livers with chronic hepatitis (CH), liver cirrhosis (LC), large regenerative nodules (LRNs), low-grade DN, high-grade DN, DN with HCC foci, and HCCs. These mRNAs were subsequently compared with the telomere length, which was measured by Southern hybridization, in multistep hepatocarcinogenesis, and then with the pathological parameters, such as the differentiation, mitotic activity, and tumor size of HCCs.

Materials and Methods

Materials and Pathological Examination

Large nodules, measuring at least 0.5 cm at their largest dimension, and appearing distinct from the surrounding cirrhotic parenchyma in terms of their color, texture, and degree of bulging at the cut surface, HCCs, and the adjacent nonneoplastic liver tissues were collected from 10 explanted livers and 28 resected specimens. The patients in this study were 23 males and 15 females with ages ranging from 32 to 74 years (mean \pm SD = 54.3 \pm 10.03). All patients tested positive to the serum HBsAg and negative to serum anti-HCV. Half of each nodule was fixed in 10% buffered formalin, routinely processed, and embedded in paraffin for a histological examination and the remaining half of each nodule was retrieved in the fresh state. The diagnosis of the tissue was confirmed by examining a frozen-sectioned slide before extraction.

The diagnostic classification of the nodular lesions was subdivided into the following five groups: 1) LRN, 2) low-grade DN, 3) high-grade DN, 4) DN with HCC foci, and 5) HCC according to the standard criteria of an international working party²³ (Figure 1). The pathology of each nodular lesion was reviewed by two hepatopathologists (Y.N.P. and C.P.). A total of 67 nodular lesions were reviewed and there were 5 LRNs, 14 low-grade DNs, 7

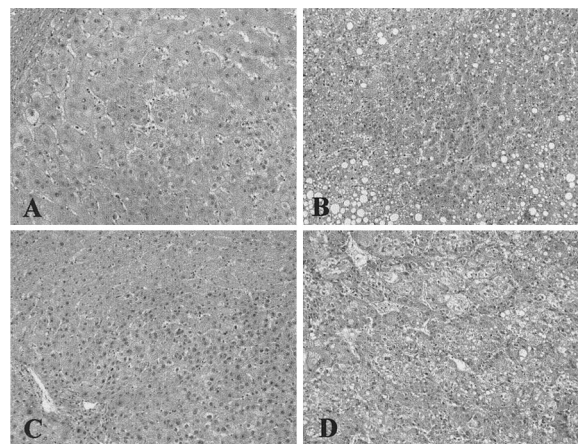


Figure 1. Microscopic feature of human multistep hepatocarcinogenesis showing low-grade DN (A), high-grade DN with small liver cell dysplasia (B), DN with HCC foci in bottom right part (C), and HCC with trabecular pattern (D). H&E; original magnifications, $\times 200$.

high-grade DN, 10 DN with HCC foci, and 31 HCCs. Eleven patients had multiple synchronous nodules ranging from 2 to 11. The differentiation of the HCC was evaluated according to the Edmondson's grading system. The differentiation of the HCC was grade I in 1, grade II in 18, and grade III in 12 HCCs. The size of the HCCs was 5.7 \pm 3.98 (mean \pm SD), ranging from 2 to 16 cm. The rate of mitosis in the HCCs was 10.6 \pm 14.83 per 10 high-power fields (mean \pm SD), ranging from 0 to 60. The background liver showed hepatitis B virus-related chronic liver disease, including 14 with CH and 24 with LC. As controls, nine normal liver tissues were obtained from the resected liver for benign lesion or metastatic carcinoma from seven male and two female patients with ages ranging from 42 to 74 years (mean \pm SD = 58.4 \pm 13.03 years). The controls tested negative for the hepatitis virus and showed a relatively normal liver histology, with the exception of a mild fatty change.

Isolation of Total RNA and Synthesis of cDNA

The frozen tissues were stored in RNAlater (Ambion, Austin, TX) at -80°C to prevent RNA degradation. The tissues, weighing 20 to 30 mg, were powdered by grinding with a pestle in liquid nitrogen. The tissue was homogenized using a Qiashredder (Qiagen, Hilden, Germany), and the total RNA was isolated using a Qiagen column, according to the manufacturer's instructions (Qiagen). The cDNA synthesis was done as previously described.³¹ The total RNA (2 μg) was pretreated with RNase-free DNase I (Takara, Shiga, Japan) for 20 minutes at 37°C to remove genomic DNA before the cDNA synthesis. The complete removal of the genomic DNA was confirmed by a PCR of the total RNA using β -actin primers, which generated no product. The cDNA synthesis was performed in a total volume of 20 μl , at 42°C for 50 minutes, containing 1 μg of the total RNA, 160 pmol of the random hexamers (Takara), 200 U of superscript RNase H⁻ reverse transcriptase (Invitrogen, Carlsbad, CA), 20 U of the RNase inhibitor (Ambion), 0.5 mmol/L

dNTP, 10 mmol/L dithiothreitol, and 1× the first strand buffer (Invitrogen). This was followed by incubation for 15 minutes at 70°C to inactivate the enzyme.

Real-Time Quantitative RT-PCR

The analyses of the TRF1, TRF2, and TIN2 mRNAs were performed using real-time quantitative RT-PCR, using an ABI Prism 7700 sequence detection system (Perkin-Elmer, Emeryville, CA), based on the TaqMan methodology. The mRNA expression levels were measured using the gene-specific fluorescent-labeled probes. Either FAM or VIC was used as the 5'-fluorescent reporters while TAMRA was added to the 3' end as a quencher. The primer and probe sequences for TRF1 are as follows: TRF1 forward primer, 5'-TCTCTCTTTGCCGAGCTTCC-3'; TRF1 reverse primer, 5'-ACTGGCAAGCTGTAGACTGGAT-3'; TRF1 probe, 5'-(FAM) CCCGCAACAGCGCAGAGGCTA (TAMRA)-3'. For the amplification of TRF2 and TIN2, gene expression products (PE Applied Biosystems, Foster City, CA) were used. The sequence of the TRF2 and TIN2 primers and probes are under the copyright of Applied Biosystems. The 18S rRNA was used to normalize the sample-to-sample variation in the amount of the input cDNA, and also to evaluate the quality of the isolated RNA and RT efficiency. Amplification of the 18S rRNA was performed using the primers and the internal probe provided by Perkin-Elmer (PE Applied Biosystems). The standard curve was constructed with fivefold serial dilutions of the cDNA from the HT1080 cell line, which corresponded to the total RNA ranging from 0.32 to 200 ng for TRF1, from 0.16 to 100 ng for TRF2, from 0.08 to 50 ng for TIN2, and from 0.008 to 5 ng for 18S rRNA. The PCR reaction for TRF1 amplification was performed using 0.5 μ l of each RT reaction, which corresponded to 25 ng of the total RNA, 1× TaqMan universal master mix (PE Applied Biosystems), 300 nmol/L of primers, and 200 nmol/L of the probe in a 25- μ l volume. The PCR reaction for TRF2 and TIN2 amplification was performed with 0.5 μ l of each RT reaction, which corresponded to 25 ng of the total RNA, 1× TaqMan universal master mix (PE Applied Biosystems), 1× each gene expression products in a 25- μ l volume. The 18S rRNA reaction was performed with 50 nmol/L of the primers, 200 nmol/L of the probe, and 1 μ l of the RT reaction, which corresponded to 0.5 ng of the total RNA. Thermal cycling was initiated with a 2-minute incubation at 50°C, for the uracil *N*-glycosylase reaction, which was followed by a 10-minute reaction at 95°C to activate the AmpliTaq gold, and 40 PCR cycles at 95°C for 15 seconds and 60°C for 1 minute. All of the measurements included a determination of the standards and no-template as a negative control, in which water was substituted for the cDNA.

Immunohistochemical Staining for TRF1

Serial sections of each lesion were immunostained with goat polyclonal anti-TRF1sc-1977 (Santa Cruz Biotechnology, Santa Cruz, CA), which recognizes the COOH terminus of TRF1. The intensity of TRF1 expression was

graded as follows: 0, none; 1, weak; 2, moderate; 3, strong. The percentage of positive cells was evaluated as follows: 0, undetectable; 1, less than 10%; 2, 10 ~ 50%; 3, more than 50%. The degree of immunopositivity was obtained by multiplying the intensity and the area of TRF1 expression, and was classified as mild with a score of 1 to 2, moderate with a score of 3 to 5, and marked with a score of 6 to 9.

Analysis of Telomere Length

The genomic DNA was prepared using the standard method, with proteinase K treatment and phenol/chloroform extraction from 10 to 50 mg of the frozen liver tissue.³⁰ Two μ g of the *Hinf*I-digested DNA were fractionated on a 0.7% agarose gel, and transferred to a nylon membrane using an upward capillary transfer. The hybridization was performed with a 3'-end digoxigenin-labeled d(TTAGGG)₄ (Roche Molecular Biochemicals, Mannheim, Germany), overnight at 37°C. The hybrids were detected according to the manufacturer's recommendation (Roche Molecular Biochemicals). The telomere length was calculated using a previously described method.³² A mean length of the sample was obtained from two to three replicate experiments.

Statistical Analysis

The values are expressed as a mean \pm SD. The statistical analyses were performed using the Mann-Whitney and linear regression tests where appropriate. A *P* value <0.05 was considered significant.

Results

Up-Regulation of TRF1, TRF2, and TIN2 in Human Multistep Hepatocarcinogenesis

The expression levels of TRF1, TRF2, and TIN2 mRNA were gradually increased according to the progression of multistep hepatocarcinogenesis and it was also evident in the patients with multiple synchronous nodules of DNAs and/or HCCs. The results are summarized in Table 1 and Figure 2. The TRF1 mRNA levels remained low in CH, LC, and LRNs, which were comparable to those of the normal liver (Table 1 and Figure 2A). The low- and high-grade DNAs expressed a higher TRF1 mRNA level than CH, LC, and LRNs (*P* = 0.002) and the mean TRF1 mRNA level of the DNAs was 1.3 times higher than that of the normal livers. TRF1 mRNA level was further increased in the DNAs with HCC foci compared to the DNAs, in which the mean value was 1.7 times higher than that of the normal livers. A marked increase was observed in the HCCs (*P* = 0.005), in which the mean value was 3.2 times higher than that of the normal livers. The HCCs showed a wide range of TRF1 mRNA level from 20 to 261, and 29 HCCs (94%) had a higher TRF1 mRNA level than the adjacent non-HCCs. According to the differentiation of HCC, those with poorer differentiation showed a significantly higher level

Table 1. Summary of the TRF1, TRF2, and TIN2 mRNA Levels and the Telomere Length in Human Multistep Hepatocarcinogenesis

	TRF1		TRF2		TIN2		Telomere length (kb)	
	Range	Mean ± SD	Range	Mean ± SD	Range	Mean ± SD	Range	Mean ± SD
Normal (n = 9)	13–42	26 ± 8.5	4–24	10 ± 7.3	3–25	12 ± 8.2	8.1–9.8	8.7 ± 0.57
CH (n = 14)	14–48	27 ± 8.8	7–29	17 ± 6.7	7–36	20 ± 9.5	6.8–9.6	8.3 ± 0.94
LC (n = 24)	15–39	28 ± 6.4	4–56	17 ± 10.8	5–49	22 ± 10.4	5.6–11.0	7.8 ± 1.19
LRN (n = 5)	23–37	30 ± 6.0	7–22	13 ± 5.5	7–15	10 ± 3.0	5.2–9.1	7.8 ± 1.63
LGDN (n = 14)	28–47	34 ± 5.9	6–29	14 ± 6.4	7–48	15 ± 11.5	3.9–9.8	7.4 ± 1.77
HGDN (n = 7)	25–38	34 ± 4.9	14–41	25 ± 9.4	19–61	32 ± 15.6	4.5–8.1	5.3 ± 1.25
DN with HCC (n = 10)	16–74	44 ± 17.2	9–58	22 ± 14.7	12–65	38 ± 20.2	4.4–8.5	6.4 ± 1.31
HCC (n = 31)	20–261	82 ± 47.4	9–92	34 ± 20.2	11–155	51 ± 29.6	4.7–14.3	7.3 ± 2.26

CH, chronic hepatitis; LC, liver cirrhosis; LRN, large regenerative nodule; LGDN, low-grade dysplastic nodule; HGDN, high-grade dysplastic nodule; DN, dysplastic nodule; HCC, hepatocellular carcinoma.
 The TRF1, TRF2, and TIN2 mRNA levels = [target gene mRNA copies of sample/18S rRNA copies of sample] × 10⁵.
 Telomere length of each tissue was obtained from two- to three replicate experiments.

of TRF1 mRNA ($P = 0.004$). However, the mitotic activity and tumor size of HCCs had no correlation with it.

The TRF1 protein expression was evaluated by immunohistochemical staining and it was found in the cytoplasm, which is consistent with a previous report.³³ The TRF1 protein expression gradually increased according to the progression of hepatocarcinogenesis and was well correlated with the TRF1 mRNA level ($P < 0.001$, $R^2 = 0.422$) (Table 2 and Figure 3).

TRF2 mRNA also appeared to increase according to the progression of multistep hepatocarcinogenesis, particularly from DNs to HCCs (Table 1 and Figure 2B). The TRF2 mRNA levels of CH and LC were higher than that of the normal liver ($P = 0.019$), however, they were still low. Low-grade DNs showed a TRF2 mRNA level similar to CH, LC, and LRNs. A significant increase was observed in the transition of the low-grade DNs to high-grade DNs ($P = 0.016$) and the mean TRF2 mRNA level of the high-grade DNs was 2.5 times higher than that of the normal livers. The DNs with HCC foci had the TRF2 mRNA level similar to high-grade DNs. A further marked increase was observed in the HCCs ($P = 0.036$), in which the mean value was 3.4 times higher than that of the normal livers. The range of TRF2 mRNA level in HCCs was a rather wide from 9 to 92 and 29 HCCs (94%) had a higher TRF2 mRNA level than the adjacent non-HCCs. TRF2 mRNA levels were significantly higher in HCCs with poorer differentiation ($P = 0.028$) and it was positively correlated with the mitotic activity of HCCs ($P < 0.001$, $R^2 = 0.347$), but had no correlation with the size of HCCs.

The TIN2 mRNA level showed a similar pattern of up-regulation during multistep hepatocarcinogenesis to TRF2 mRNA (Table 1 and Figure 2C). CH and LC expressed TIN2 mRNA at a similarly low level, although their expression level was higher than that of the normal liver ($P = 0.043$). Low-grade DNs showed a similar TIN2 mRNA level to that observed in the livers with CH and LC. A significant increase was noted in the transition from the low-grade DNs to high-grade DNs ($P = 0.007$) and the mean value of the high-grade DNs was 2.7 times higher than the normal livers. A further increase was observed in the DNs with HCC foci, in which the mean value was 3.2 times higher than that of the normal livers. The HCCs

showed a marked increase in the TIN2 mRNA level ($P = 0.026$), in which the mean value was 4.3 times higher than that of the normal livers. All of the HCCs expressed a higher amount of TIN2 than the adjacent non-HCC, and their TIN2 mRNA level ranged from 11 to 155. TIN2 mRNA level showed a positive correlation with mitotic activity of HCCs ($P < 0.001$, $R^2 = 0.424$), however it showed no significant difference according to the differentiation and size of HCCs. The TRF1, TRF2, and TIN2 mRNA levels appeared to positively correlate with each other. The TRF1 mRNA levels were higher in the lesions with higher TRF2 ($P < 0.001$, $R^2 = 0.377$) and TIN2 levels ($P < 0.001$, $R^2 = 0.323$), and a similar feature was found between TRF2 and TIN2 ($P < 0.001$, $R^2 = 0.547$).

Telomere Shortening during Human Multistep Hepatocarcinogenesis

The normal liver tissues showed telomere lengths ranging from 8.1 to 9.8 kb, which did not significantly correlate with the patient ages. A gradual reduction in the telomere length was observed from the livers with CH, to LC, and to LRNs (Table 1 and Figure 4). The low-grade DNs had a wide range of telomere lengths, most of which showed similar telomere length to those with CH, LC, and LRNs, and two (14%) of the low-grade DNs had short telomeres, which overlapped with those of the high-grade DNs. Significant telomere shortening occurred in the transition of the low-grade DNs to high-grade DNs ($P = 0.020$). The high-grade DNs showed telomere lengths ranging from 4.5 to 8.1 kb, and six (86%) of those had a telomere length <5.4 kb. DNs with HCC foci had telomere length in the similar range to those of high-grade DNs. The HCCs had a telomere length with a wide range from 4.7 to 14.3 kb and showed no significant reduction of the telomere length compared to those of DNs with HCC foci, but most HCCs (24 of 31, 77%) had shorter telomeres than their adjacent non-HCCs.

Most nodular lesions (52 of 67, 78%) including 4 LRNs, 11 low-grade DNs, 7 high-grade DNs, 6 DNs with HCC foci, and 24 HCCs had shorter telomeres

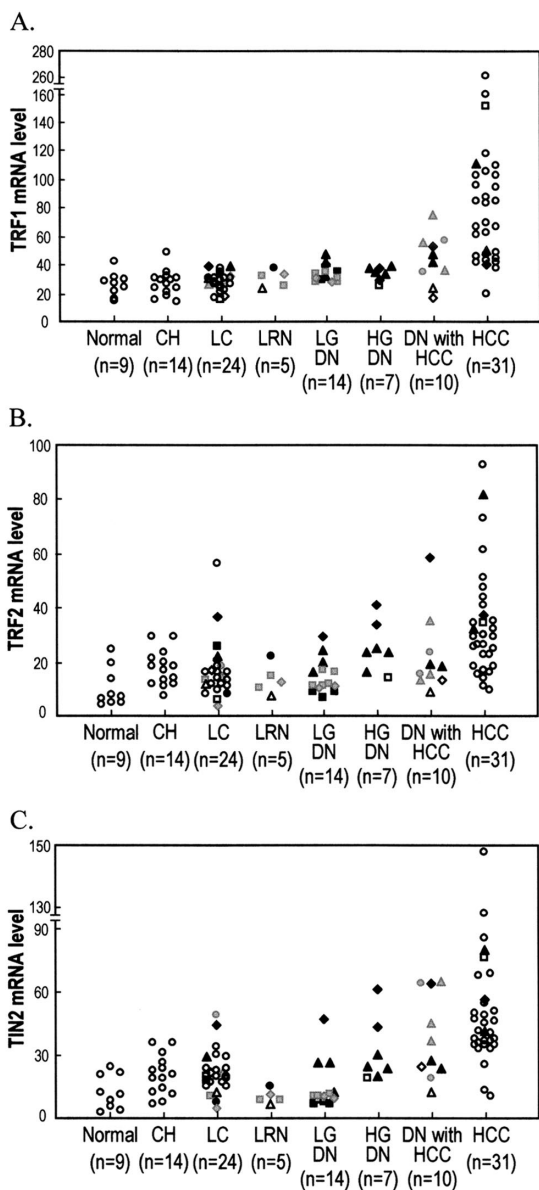


Figure 2. Comparison of the TRF1, TRF2, and TIN2 mRNA levels in human multistep hepatocarcinogenesis. The TRF1 (A), TRF2 (B), and TIN2 (C) mRNA levels are shown in normal livers, CH, LC, LRNs, low-grade dysplastic nodules (LGDNs), high-grade dysplastic nodules (HGDNs), DNs with HCC foci, and HCCs. Eleven patients with multiple synchronous nodules are denoted by different symbols according to the patient numbers (patient 1, **black square**; patient 2, **black diamond**; patient 3, **black triangle**; patient 4, **black circle**; patient 5, **gray square**; patient 6, **gray diamond**; patient 7, **gray triangle**; patient 8, **gray circle**; patient 9, **white square**; patient 10, **white diamond**; patient 11, **white triangle**; others, **white circle**).

than their adjacent CH/LC, whereas some lesions (15 of 67, 22%) including a LRN, 3 low-grade DNs, 4 DNs with HCC foci, and 7 HCCs had longer telomeres. Three of the HCCs had telomeres >10 kb. A case of HCC with a telomere length of 14.3 kb is believed to be an alternative lengthening of the telomere because it possessed neither telomerase activity nor hTERT mRNA (data not shown).

Table 2. Semiquantitative Assessment of TRF1 Protein Expression in Human Multistep Hepatocarcinogenesis

	Mild	Moderate	Marked
Normal (<i>n</i> = 9)	8	1	0
CH (<i>n</i> = 14)	11	3	0
LC (<i>n</i> = 24)	22	2	0
LRN (<i>n</i> = 5)	4	1	0
LGDN (<i>n</i> = 14)	8	6	0
HGDN (<i>n</i> = 7)	3	4	0
DN with HCC (<i>n</i> = 10)	0	8	2
HCC (<i>n</i> = 31)	0	4	27

CH, chronic hepatitis; LC, liver cirrhosis; LRN, large regenerative nodule; LGDN, low-grade dysplastic nodule; HGDN, high-grade dysplastic nodule; DN, dysplastic nodule; HCC, hepatocellular carcinoma.

TRF1, TRF2, and TIN2 in Relation to Telomere Length Regulation

To evaluate whether TRF1, TRF2, and TIN2 are involved in the telomere length regulation, the mRNA levels of these genes were compared with the telomere length in each lesion. All of these genes showed significant negative correlations with the telomere length, when the analysis was done with the lesions with shortened telomeres compared to their respective adjacent CH and LC (note: this analysis included 4 LRNs, 11 low-grade DNs, 7 high-grade DNs, 6 DNs with HCC foci, 24 HCCs, and their respective adjacent CH and LC) (Figure 5). The inverse correlation was more evident in the early stages of hepatocarcinogenesis including low-grade DNs, high-grade DNs, and DNs with HCC foci ($P = 0.036$, $R^2 = 0.184$; $P = 0.002$, $R^2 = 0.352$; $P = 0.005$, $R^2 = 0.308$, respectively). Meanwhile, there was no statistically significant relationship between those genes and the telomere length in the HCCs, which showed a rather wide range of mRNA levels of these genes.

The analysis was also performed on the nodular lesions with the lengthened telomeres compared to the respective adjacent CH and LC, which were one LRN, three low-grade DNs, four DNs with HCC foci, and seven

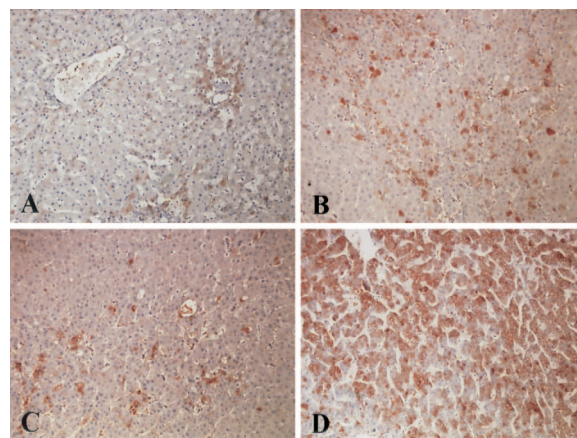


Figure 3. Immunoreactivity of TRF1. TRF1 protein expression is mild in CH (A), moderate in high-grade dysplastic nodule (B), and further increased in DN with HCC foci (C) with the marked expression in HCC (D). Notice that increased TRF1 protein expression with the progression of human multistep hepatocarcinogenesis. Original magnifications, $\times 200$.

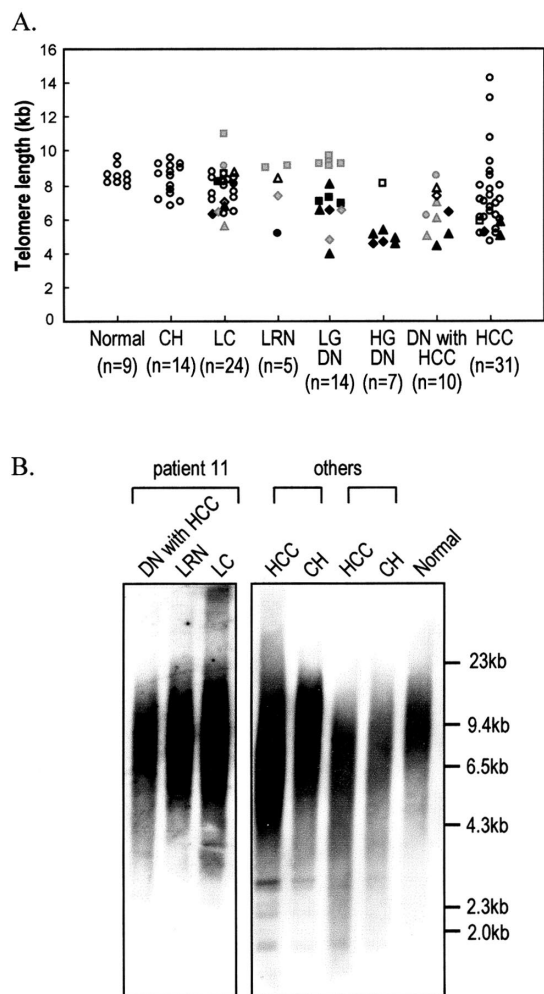


Figure 4. Comparison of the telomere length in human multistep hepatocarcinogenesis. **A:** The telomere length is shown in normal livers, CH, LC, LRNs, low-grade dysplastic nodules (LGDNs), high-grade dysplastic nodules (HGDNs), DNs with HCC foci, and HCCs. The lesions are denoted by different symbols according to the patient numbers (patient 1, **black square**; patient 2, **black diamond**; patient 3, **black triangle**; patient 4, **black circle**; patient 5, **gray square**; patient 6, **gray diamond**; patient 7, **gray triangle**; patient 8, **gray circle**; patient 9, **white square**; patient 10, **white diamond**; patient 11, **white triangle**; others, **white circle**). **B:** A representative result of Southern blot analysis in various lesions. The genomic DNA, digested with *Hin*I, was hybridized with a digoxigenin-labeled d(TTAGGG)_n. The mean telomere restriction fragment length was calculated by a previously described method,³² using the Image Gauge software (Fujifilm, Tokyo, Japan). The size markers are indicated on the **right**.

HCCs. Most of these lesions also expressed higher levels of TRF1, TRF2, and TIN2 mRNA compared to the respective adjacent CH and LC. However, the mRNA levels of these genes did not show a significant correlation with the telomere length in the lesions with elongated telomeres.

Discussion

In this study, up-regulation of TRF1, TRF2, and TIN2 mRNA levels was observed according to the progression of human multistep hepatocarcinogenesis, particularly from DNs to HCCs. A similar expression pattern was observed in TRF1 protein. To evaluate whether up-regulation of these genes is a common pathway in hepato-

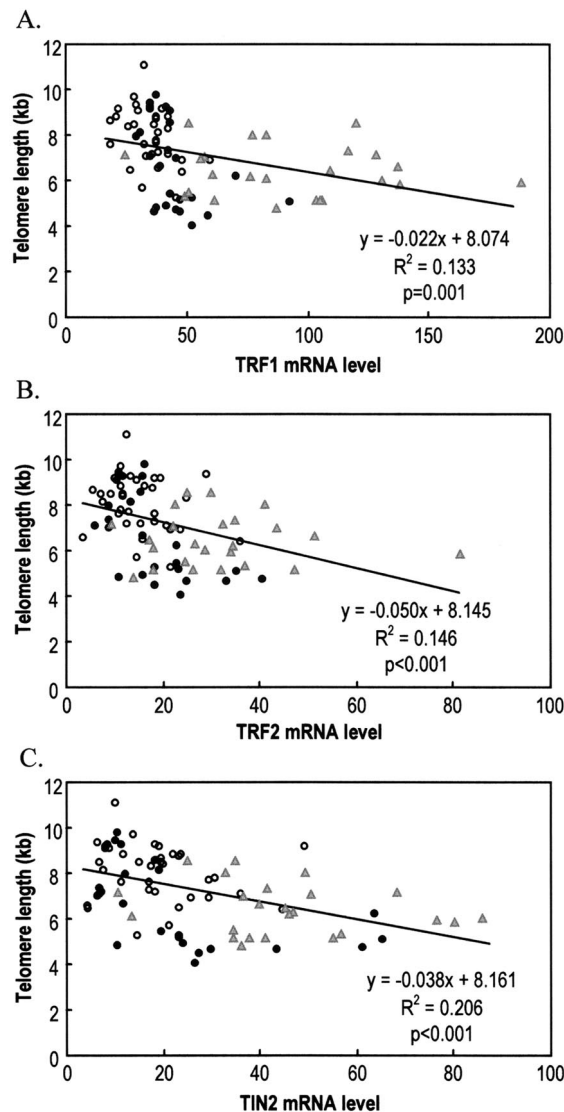


Figure 5. Comparison of TRF1, TRF2, and TIN2 mRNA levels with the telomere length in human multistep hepatocarcinogenesis. The TRF1, TRF2, and TIN2 mRNA levels are compared with the telomere length, shown in **A**, **B**, and **C**, respectively. The analysis was performed with the nodular lesions with shortened telomeres compared to the adjacent CH and LC. This analysis included 4 LRNs, 11 low-grade dysplastic nodules (DNs), 7 high-grade DNs, 6 DNs with HCC foci, 24 HCCs, and their respective adjacent CH ($n = 11$) and LC ($n = 19$). CH, LC, and LRNs are indicated with **white circles**, low- and high-grade DNs and DNs with HCC foci with **black circles**, and HCCs with **gray triangles**.

carcinogenesis regardless of its etiology, their mRNA levels were examined in seven HCCs related to hepatitis C virus or alcohol and their adjacent non-HCCs (data not shown). This analysis showed a similar up-regulation of these genes in the HCCs compared to their adjacent non-HCCs, which indicates that TRF1, TRF2, and TIN2 up-regulation might be a general mechanism of hepatocarcinogenesis.

This study demonstrated progressive telomere shortening according to the progression of hepatocarcinogenesis. Most (78%, 52 of 67) of the nodular lesions including LRNs, DNs, and HCCs had shorter telomeres than their adjacent CH/LC, and the lesions with shorter telomeres had a higher mRNA expression level of TRF1, TRF2, and

TIN2. This inverse correlation suggested that these telomere-binding proteins play important roles in telomere shortening during multistep hepatocarcinogenesis. Moreover, the positive correlations among the expression levels of these genes suggest their collaboration in telomere shortening. It was proposed that these telomere-binding proteins act as negative length regulators at the telomeres.^{12,14,34-37} During hepatocarcinogenesis, telomere shortening occurred despite telomerase activation.³⁰ This might be, in part, explained as follows: the up-regulation of TRF1, TRF2, and TIN2 might be involved in the stabilization of the telomeres by promoting t-loop folding. The stabilization of the t-loop structures, which limits the access of telomerase to the telomeres,^{36,37} would eventually result in telomere shortening in hepatocarcinogenesis.

There is growing evidence that DNs are precancerous lesions.³⁸ Previous studies as well as this study have demonstrated that many of high-grade DNs have a short telomere length and a high telomerase activity, which is similar to those of HCCs. Moreover, some low-grade DNs also have similar features.³⁰ Considering that telomere shortening and telomerase activation play a key role in tumorigenesis, these results suggest that low- and high-grade DNs are important early lesions in multistep hepatocarcinogenesis. Telomere shortening leads to loss of telomere capping, chromosomal fusion, and chromosomal instability, which generate a variety of aberrant chromosomes without functional telomeres at the chromosomal ends via a mechanism of breakage-fusion-bridge cycle, and cells with aberrant chromosomes would eventually die unless broken chromosome ends are healed by telomerase.³⁹ Interestingly, telomere reduction and telomerase activation are evident in most early lesions of hepatocarcinogenesis such as high-grade DNs and DNs with HCC.³⁰ Thus, it is believed that these lesions maintain an active end-healing mechanism, thereby they can provide stable and aberrant chromosomes. In fact, chromosomal aberration is reported in the early lesions of hepatocarcinogenesis and HCCs have a high incidence of chromosomal instability.⁴⁰ In this study, a significant increase of TRF1, TRF2, and TIN2 expression and an inverse correlation between mRNA levels of these genes and the telomere length were first noted in DNs during multistep hepatocarcinogenesis. These results suggest that these telomere-binding proteins are involved in telomere shortening in the early stages of hepatocarcinogenesis. Up-regulation of these genes, therefore, is likely to be crucial for hepatocarcinogenesis by inducing telomere crisis, a driving force in tumor development.³⁹

HCCs showed no further significant telomere shortening, compared to the high-grade DNs and DNs with HCC foci. One of the possible explanations for this would be the expression of strong telomerase in the HCCs.^{24,25,30} HCCs expressed a high TRF1, TRF2, and TIN2 mRNA level, and their mean value was more than three to four times that of the normal livers. The mRNA levels of these genes showed no significant correlation with telomeres in HCCs, indicating that the induction of these genes is unlikely to directly influence telomere shortening in the

HCCs. Their roles on telomere shortening might be screened by the strong telomerase activity, which is involved in telomere elongation. Therefore, the balance between the telomere-binding protein expression and telomerase activation might be crucial for the telomere maintenance in HCCs. Interestingly, the HCCs with poorer differentiation or higher mitotic activity expressed higher mRNA levels of these telomere-binding protein genes. This suggests that an excess of these genes is likely to be involved in HCC progression.

Telomere lengthening was also found during hepatocarcinogenesis. Seven HCCs and eight other nodular lesions showed an elongated telomere length. It suggests that the mechanism of telomere lengthening is also involved in hepatocarcinogenesis, even though it is a minor pathway. Our data on higher levels of TRF1, TRF2, and TIN2 mRNA in those lesions but no correlation with telomere length suggest that an excess of these genes might be required for the association with the lengthened telomeres rather directly involved in telomere length regulation.

In conclusion, an up-regulation of TRF1, TRF2, and TIN2 was observed during multistep hepatocarcinogenesis and mRNA levels of these genes inversely correlated with the telomere length. The negative correlation was more evident in the DNs and DNs with HCC foci of early stages of hepatocarcinogenesis in which the telomere was significantly shortened. These findings suggest that TRF1, TRF2, and TIN2 are involved in hepatocarcinogenesis, particularly in the early stages of hepatocarcinogenesis by playing crucial roles in the telomere shortening.

Acknowledgments

We thank Mr. Chan-Hee Lee for his technical assistance with immunostaining and Dr. Yhong-Hee Shim for critical comments on the manuscript.

References

1. Wright JH, Gottschling DE, Zakian VA: Saccharomyces telomeres assume a non-nucleosomal chromatin structure. *Genes Dev* 1992, 6:197-210
2. Tommerup H, Dousmanis A, de Lange T: Unusual chromatin in human telomeres. *Mol Cell Biol* 1994, 14:5777-5785
3. Nugent CI, Hughes TR, Lue NF, Lundblad V: Cdc13p: a single-strand telomeric DNA-binding protein with a dual role in yeast telomere maintenance. *Science* 1996, 274:249-252
4. Karlseder J: Telomere repeat binding factors: keeping the ends in check. *Cancer Lett* 2003, 194:189-197
5. Collins K: Mammalian telomeres and telomerase. *Curr Opin Cell Biol* 2000, 12:378-383
6. Blackburn EH: Switching and signaling at the telomere. *Cell* 2001, 106:661-673
7. Kim SH, Kaminker P, Campisi J: Telomeres, aging and cancer: in search of a happy ending. *Oncogene* 2002, 21:503-511
8. Hackett JA, Greider CW: Balancing instability: dual roles for telomerase and telomere dysfunction in tumorigenesis. *Oncogene* 2002, 21:619-626
9. Griffith JD, Comeau L, Rosenfield S, Stansel RM, Bianchi A, Moss H, de Lange T: Mammalian telomeres end in a large duplex loop. *Cell* 1999, 97:503-514
10. Stansel RM, de Lange T, Griffith JD: T-loop assembly in vitro involves

- binding of TRF2 near the 3' telomeric overhang. *EMBO J* 2001, 20:5532–5540
11. van Steensel B, de Lange T: Control of telomere length by the human telomeric protein TRF1. *Nature* 1997, 385:740–743
 12. Smogorzewska A, van Steensel B, Bianchi A, Oelmann S, Schaefer MR, Schnapp G, de Lange T: Control of human telomere length by TRF1 and TRF2. *Mol Cell Biol* 2000, 20:1659–1668
 13. van Steensel B, Smogorzewska A, de Lange T: TRF2 protects human telomeres from end-to-end fusions. *Cell* 1998, 92:401–413
 14. Kim SH, Kaminker P, Campisi J: TIN2, a new regulator of telomere length in human cells. *Nat Genet* 1999, 23:405–412
 15. Smith S, Giriati I, Schmitt A, de Lange T: Tankyrase, a poly(ADP-ribose) polymerase at human telomeres. *Science* 1998, 282:1484–1487
 16. Li B, Oestreich S, de Lange T: Identification of human Rap1: implications for telomere evolution. *Cell* 2000, 101:471–483
 17. Nakanishi K, Kawai T, Kumaki F, Hiroi S, Mukai M, Ikeda E, Koering CE, Gilson E: Expression of mRNAs for telomeric repeat binding factor (TRF)-1 and TRF2 in atypical adenomatous hyperplasia and adenocarcinoma of the lung. *Clin Cancer Res* 2003, 9:1105–1111
 18. Miyachi K, Fujita M, Tanaka N, Sasaki K, Sunagawa M: Correlation between telomerase activity and telomeric-repeat binding factors in gastric cancer. *J Exp Clin Cancer Res* 2002, 21:269–275
 19. Klapper W, Krams M, Qian W, Janssen D, Parwaresch R: Telomerase activity in B-cell non-Hodgkin lymphomas is regulated by hTERT transcription and correlated with telomere-binding protein expression but uncoupled from proliferation. *Br J Cancer* 2003, 89:713–719
 20. Saito K, Yagihashi A, Nasu S, Izawa Y, Nakamura M, Kobayashi D, Tsuji N, Watanabe N: Gene expression for suppressors of telomerase activity (telomeric-repeat binding factors) in breast cancer. *Jpn J Cancer Res* 2002, 93:253–258
 21. Yamada M, Tsuji N, Nakamura M, Moriai R, Kobayashi D, Yagihashi A, Watanabe N: Down-regulation of TRF1, TRF2 and TIN2 genes is important to maintain telomeric DNA for gastric cancers. *Anticancer Res* 2002, 22:3303–3307
 22. Yamada K, Yagihashi A, Yamada M, Asanuma K, Moriai R, Kobayashi D, Tsuji N, Watanabe N: Decreased gene expression for telomeric-repeat binding factors and TIN2 in malignant hematopoietic cells. *Anticancer Res* 2002, 22:1315–1320
 23. International Working Party: Terminology of nodular hepatocellular lesions. *Hepatology* 1995, 22:983–993
 24. Miura N, Horikawa I, Nishimoto A, Ohmura H, Ito H, Hirohashi S, Shay JW, Oshimura M: Progressive telomere shortening and telomerase reactivation during hepatocellular carcinogenesis. *Cancer Genet Cytogenet* 1997, 93:56–62
 25. Huang GT, Lee HS, Chen CH, Chiou LL, Lin YW, Lee CZ, Chen DS, Sheu JC: Telomerase activity and telomere length in human hepatocellular carcinoma. *Eur J Cancer* 1998, 34:1946–1949
 26. Hytiroglou P, Kotoula V, Thung SN, Tsokos M, Fiel MI, Papadimitriou CS: Telomerase activity in precancerous hepatic nodules. *Cancer* 1998, 82:1831–1838
 27. Kitamoto M, Ide T: Telomerase activity in precancerous hepatic nodules. *Cancer* 1999, 85:245–248
 28. Isokawa O, Suda T, Aoyagi Y, Kawai H, Yokota T, Takahashi T, Tsukada K, Shimizu T, Mori S, Abe Y, Suzuki Y, Nomoto M, Mita Y, Yanagi M, Igarashi H, Asakura H: Reduction of telomeric repeats as a possible predictor for development of hepatocellular carcinoma: convenient evaluation by slot-blot analysis. *Hepatology* 1999, 30:408–412
 29. Youssef N, Paradis V, Ferlicot S, Bedossa P: In situ detection of telomerase enzymatic activity in human hepatocellular carcinogenesis. *J Pathol* 2001, 194:459–465
 30. Oh BK, Chae KJ, Park C, Kim K, Lee WJ, Han KH, Park YN: Telomere shortening and telomerase reactivation in dysplastic nodules of human hepatocarcinogenesis. *J Hepatol* 2003, 39:786–792
 31. Oh BK, Seong JK, Lee JE, Chae KJ, Roh KJ, Park C, Park YN: Induction of telomerase activity during an early burst of proliferation in pancreatic regeneration. *Cancer Lett* 2002, 186:93–98
 32. Kruk PA, Rampino NJ, Bohr VA: DNA damage and repair in telomeres: relation to aging. *Proc Natl Acad Sci USA* 1995, 92:258–262
 33. Igarashi M, Suda T, Hara H, Takimoto M, Nomoto M, Takahashi T, Okoshi S, Kawai H, Mita Y, Waguri N, Aoyagi Y: Interferon can block telomere erosion and in rare cases result in hepatocellular carcinoma development with telomeric repeat binding factor 1 overexpression in chronic hepatitis C. *Clin Cancer Res* 2003, 9:5264–5270
 34. Ancelin K, Brunori M, Bauwens S, Koering CE, Brun C, Ricoul M, Pommier JP, Sabatier L, Gilson E: Targeting assay to study the cis functions of human telomeric proteins: evidence for inhibition of telomerase by TRF1 and for activation of telomere degradation by TRF2. *Mol Cell Biol* 2002, 22:3474–3487
 35. Kim SH, Han S, You YH, Chen DJ, Campisi J: The human telomere-associated protein TIN2 stimulates interactions between telomeric DNA tracts in vitro. *EMBO Rep* 2003, 4:685–691
 36. Ancelin K, Brun C, Gilson E: Role of the telomeric DNA-binding protein TRF2 in the stability of human chromosome ends. *Bioessays* 1998, 20:879–883
 37. Karlseder J, Smogorzewska A, de Lange T: Senescence induced by altered telomere state, not telomere loss. *Science* 2002, 295:2446–2449
 38. Theise ND, Park YN, Kojiro M: Dysplastic nodules and hepatocarcinogenesis. *Clinical Liver Disease. Liver Histopathology*. Edited by JH Lefkowitz. Philadelphia, W.B. Saunders, 2002, pp 497–512
 39. Ishikawa F: Breakthrough and views. Telomere crisis, the driving force in cancer cell evolution. *Biochem Biophys Res Commun* 1997, 230:1–6
 40. Nishida N, Nishimura T, Ito T, Komeda T, Fukuda Y, Nakano K: Chromosomal instability and human hepatocarcinogenesis. *Histol Histopathol* 2003, 18:897–909